Low-Frequency Response of Accelerometers for Observer Design in a Gravity Environment

M. A. Norris*
Virginia Polytechnic Institute and State University, Blacksburg, Virginia 24061
R. C. Thompson†
Pennsylvania State University, University Park, Pennsylvania 16802
and
A. Das‡
Air Force Astronautics Laboratory, Edwards Air Force Base, Edwards, California 93523

Analytical and experimental results demonstrate that the dynamic effect of gravity degrades low-frequency accelerometer measurements. The attitude of an accelerometer in motion in a constant uniform gravity field can cause the output signal to indicate an incorrect amplitude (magnitude and phase) relative to the actual acceleration of the point on the structure at which the sensor is mounted. The effect of gravity is to attenuate the accelerometer signals to the extent that a 180-deg phase shift between signals at different locations may occur in the lower modes of vibration. The positions on the structure where the phase shift occurs are called accelerometer nodal locations, because the output of accelerometers located at these positions are theoretically zero. The effect is demonstrated analytically and experimentally when results from a pendulum and a two-dimensional grid structure are used. An observer is designed for the grid structure in which accelerometer measurements are used as input. The observer performance, including the dynamic effect of gravity on the accelerometer, is compared to the performance of an observer using the output signal from the accelerometers without compensating for the signal errors induced by the gravity field. The results show that the dynamic effect of gravity must be included in the observer design for low-frequency response estimates in a gravity environment.

Introduction

MANEUVER and vibration suppression strategies for flexible structures have received considerable attention in recent years. Numerous identification and control techniques have been proposed for active vibration suppression of large space structures (LSS).[1-9] To test and evaluate the techniques, ground experiments must be performed to determine their practicality, performance, and robustness. The techniques require sensors to estimate the state of the structure to be used for identification and control strategies. Furthermore, in the test and evaluation phase, it is desirable to use sensors that are suitable for space environment, so that the identification and control techniques can be evaluated under realistic constraints. Accelerometers have been proposed for use in active vibration and flutter suppression systems to control flexible structures.[8-10]

The wide variety of sensors used to estimate the state of the structure includes strain gages, rate gyros, accelerometers, embedded sensors, proximity sensors, and piezoelectric distributed (film) sensors. In this paper, we focus our attention on the application of accelerometers, and results are reported accordingly. We do not imply that any one type of sensor is more suitable than another. The accelerometer may be advantageous for active vibration suppression of flexible structures, due to its small size and low weight. In addition, the piezoelectric and piezoresistive accelerometers are becoming increasingly popular, due to recent improvements in sensitivity to low-frequency response and weight reduction. With the enhanced capability in the low-frequency range, the accelerometer may be used to measure the low-frequency response of flexible space structures. Results reported in this paper indicate that the dynamic effect of gravity is to degrade low-frequency accelerometer measurements.

We considered the applications of accelerometer measurements on a rigid-body and a two-dimensional grid structure in a 1-g environment, in which the accelerometers are used to measure the transverse vibration of the structure relative to its static equilibrium position. The ground experiments were conducted at the Air Force Astronautics Laboratory (AFAL), LSS laboratory. The AFAL experimental facility is used to verify and develop identification and control strategies for flexible structures.[8] Currently, structural vibrations are monitored using high-sensitivity low-mass piezoelectric accelerometers and proximity sensors. Initial results support the use of accelerometer measurements for ground-based testing of identification and control techniques.

At low structural vibration frequencies in a gravity environment, the output of the accelerometers can provide unexpected results. As one might expect, the amplitude of the accelerometer output is dependent on the location of the accelerometer on the structure. The attitude of the accelerometer in the gravity field is sensed as a component of acceleration and consequently will be reflected in the output signal. For the case in which an accelerometer is mounted on a rigid structure in pendulum motion, the accelerometer signal is attenuated by the gravitational component and can be zero at a specific location on the pendulum. We call this location the accelerometer nodal location. For elastic motion of a structure, acceler-

Received Sept. 9, 1988; revision received March 7, 1989.

*Assistant Professor, Department of Engineering Science and Mechanics. Member AIAA.
†Assistant Professor, Department of Aerospace Engineering. Member AIAA.
‡Aerospace Engineer. Member AIAA.

ometer nodal locations can be determined for certain modes of vibration and predominantly occur in the lower modes of vibration. For the two-dimensional grid, the effect of gravity is to attenuate the accelerometer signals and to produce an apparent 180-deg phase shift in the accelerometer output for the first mode of vibration (when comparing accelerometer outputs vertically above and below this nodal location). The apparent 180-deg phase shift is due to the incorrect sign caused by the component of gravity. Indeed, gravity alters the magnitude and sign of the accelerometer signal from its expected output, but does not cause arbitrary phase errors in the signal. In addition, the attenuation of the accelerometer measurements degrades the identification of the mode shapes of the grid, in which identification of the first mode shape is especially poor.

This paper illustrates the dynamic effect of gravity on low-frequency accelerometer measurements, where the accelerometer translates and rotates in a constant, uniform gravity environment. The results are verified through analysis and experiment. The paper introduces the phenomenon by describing the accelerometer output for the case of pendulum motion. After introducing the equations of motion for flexible structures, the accelerometer nodal locations are determined analytically for elastic motion. To circumvent the gravity effect on the accelerometer output, an observer can be implemented as long as it includes an accurate mathematical model of the structure and the mathematical model of the gravity effect on the sensors. The observer outputs are compared with and without the gravitational effect in the design. When the gains of the observer are chosen to satisfy the Riccati equation for stochastic signals, the observer is known as a Kalman filter. Analytical and experimental results, using the pendulum and the two-dimensional grid structure, illustrate the gravity effect on the accelerometer signals.

Accelerometers in Pendulum Motion

We begin with the mechanical representation of a vibration measuring instrument, as shown in Fig. 1.[11-13] The mass, damping, and spring stiffness of the instrument are denoted m, c, and k, respectively. The displacement of the case, the displacement of the mass relative to the case, and the absolute displacement of the mass are denoted by $y(t)$, $z(t)$, and $x(t)$, respectively, so that $x(t) = y(t) + z(t)$. The relative displacement $z(t)$ is measured and the measurement is used to infer the motion $y(t)$ of the case. From Newton's second law, the equation of motion can be written as[11]

$$m\ddot{x}(t) + c[\dot{x}(t) - \dot{y}(t)] + k[x(t) - y(t)] = 0 \tag{1}$$

which, upon eliminating $x(t)$, becomes

$$m\ddot{z}(t) + c\dot{z}(t) + kz(t) = -m\ddot{y}(t) \tag{2}$$

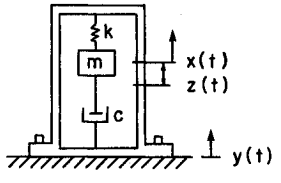

Fig. 1 Vibration measuring instrument.

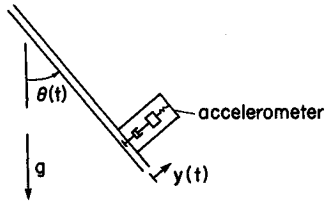

Fig. 2 Accelerometer in pendulum motion.

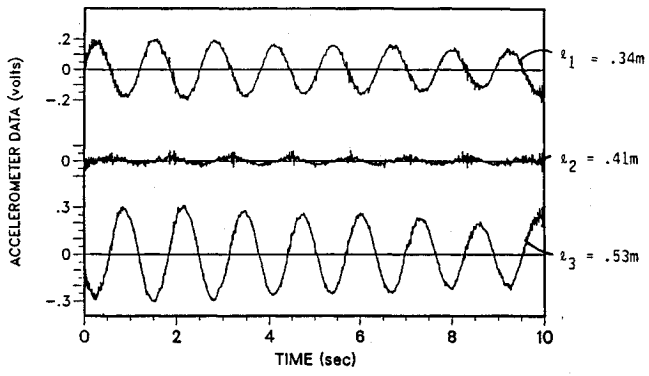

Fig. 3 Accelerometer outputs for pendulum motion.

Note that the gravitational component of acceleration can be ignored as Eqs. (1) and (2) describe motion about the equilibrium position, where gravity is considered to be a static effect. The accelerometer parameters, m, c, and k, are designed such that $\omega \ll \omega_n$, where ω and ω_n denote the excitation frequency and the natural frequency of oscillation of the accelerometer, respectively. For harmonic motion of the case $y(t)$, it can be shown that Eq. (2) becomes[13]

$$\omega_n^2 z \cong \omega^2 y \tag{3}$$

Hence, by measuring z and knowing ω_n, the acceleration of the case $\ddot{y} \cong -\omega_n^2 z$ can be determined.

Consider an accelerometer translating and rotating in a gravitational field (Fig. 2). As will become evident, gravity will no longer be considered a static effect. From Newton's second law, Eq. (2) now has the form

$$m\ddot{z}(t) + c\dot{z}(t) + kz(t) = -m\ddot{y}(t) - mg\sin\theta(t) \tag{4}$$

We consider the application in which the accelerometer is mounted to estimate the tangential component of acceleration along a rigid structure in pendulum motion. The tangential acceleration of the accelerometer casing is then $\ddot{y} = \ell\ddot{\theta}$, where ℓ represents the radial distance from the accelerometer to the pendulum support. When the small angle approximation $\sin\theta = y/\ell$ is used, Eq. (4) becomes

$$m\ddot{z} + c\dot{z} + kz = -m\left(\ddot{y} + \frac{g}{\ell}\right) y \tag{5}$$

Where we note that in pendulum motion, the angular displacement $\theta(t)$ and the tangential accelerations $\ddot{y}$ are harmonic with frequency ω. It is now obvious that the acceleration due to gravity is no longer a static effect for small pendulum motion of the accelerometer. Hence, in the case of pendulum motion, Eq. (3) becomes

$$\omega_n^2 z \cong \left(\omega^2 - \frac{g}{\ell}\right) y \tag{6}$$

Equation (6) indicates that the dynamic effect of gravity is to reduce the output (signed amplitude) of the accelerometer. Figure 3 displays experimental results of three piezoelectric accelerometers mounted on a rigid bar in pendulum motion. The natural frequency of vibration of the pendulum, obtained experimentally, is $\omega = 4.9$ rad/s. The three accelerometers are placed at locations $\ell_1 = 0.34$ m, $\ell_2 = 0.41$ m, and $\ell_3 = 0.53$ m, respectively, along the rigid bar. Note that the output of the accelerometer at location ℓ_2 is nearly zero because $\ell_2 \cong g/\omega^2$, which designates the accelerometer nodal location for the pendulum. In addition, note the 180-deg phase difference between the output of accelerometers located at ℓ_1 and ℓ_3.

For structures in elastic vibration, the dynamic effect of gravity may also disturb the output of the accelerometers. For

elastic motion, we resort to the equations of motion to determine the relationship between the translation and rotation of the accelerometer. Indeed, accelerometer nodal locations for structures in elastic motion can be found using the equations of motion governing the structures, and they can be found for the modes of vibration individually. In the next section, we present the equations of motion for structures in elastic vibration.

Equations of Motion for Structures

The equations of motion of a flexible structure can be written in the form of a partial differential equation[14]

$$Lu(P,t) + m(P)\ddot{u}(P,t) = f(P,t), \qquad P \in D \tag{7}$$

where $u(P,t)$ is the displacement of a point P in the domain D, $m(P)$ is the mass density, and $f(P,t)$ is the external force density. We consider the case in which the centrifugal forces can be ignored such that L is a self-adjoint positive-definite differential operator representing the system stiffness. Moreover, we assume that structural damping and gyroscopic forces are small enough to be neglected. The displacement u must satisfy prescribed boundary conditions. Associated with Eq. (7), we have the differential eigenvalue problem

$$L\phi(P) = \lambda m(P)\phi(P) \tag{8}$$

in which $\phi(P)$ satisfies the prescribed boundary conditions. The solution to Eq. (8) consists of a denumerably infinite set of real eigenfunctions $\phi_r(P)$ and associated real, positive eigenvalues λ_r, which represent the mode shapes and square of the natural frequencies of oscillation, respectively. The infinite set of eigenfunctions are spatially orthogonal and can be normalized to satisfy the orthonormality conditions.[14] Using the expansion theorem[14]

$$u(P,t) = \sum_{r=1}^{\infty} \phi_r(P) q_r(t) \tag{9}$$

and the orthonormality conditions, we can transform the equations of motion [Eqs. (7)] into an infinite set of independent second-order ordinary differential modal equations

$$\ddot{q}_r(t) + \omega_r^2 q_r(t) = f_r(t), \qquad r = 1,2,\ldots \tag{10}$$

where $\omega_r^2 = \lambda_r$, ω_r represent the natural frequencies of oscillation, and $f_r(t)$ are modal forces given by

$$f_r(t) = \int_D \phi_r(P) f(P,t)\, dD \tag{11}$$

Nodal Locations for Vibration-Measuring Instruments

In this section, we derive the accelerometer nodal locations for structures in elastic vibration, or nodal locations for any vibration-measuring instrument in which Eq. (4) holds. Before obtaining the nodal locations, we note that Eqs. (5) and (6) were obtained using the kinematic relations between the tangential and angular acceleration and assuming small motions of the pendulum about the static equilibrium position. For structures in elastic vibration, we use the equations of motion of the structure to obtain the relation between the transverse displacement y and the angular displacement $\theta(t)$.

In the linear range, the displacement of the structure is small enough that we can assume the accelerometer signal $\ddot{y}$ coincides with the transverse acceleration $\ddot{u}_i = \ddot{u}(P_i,t)$ $(i = 1,2,\ldots,m)$ at a point P_i denoting the ith accelerometer location. Moreover, u_i represents the displacement from the static equilibrium position of the structure at a point P_i, so that $\theta(t)$ in Eq. (4) represents any nominal rotation about the equilibrium point and is equal to u_i' $(i = 1,2,\ldots,m)$, as illustrated in Fig. 4, which is the local slope at P_i with respect to the static equilibrium position. Hence, Eq. (4) becomes

$$m\ddot{z}_i + c\dot{z}_i + kz_i = -m\ddot{u}_i - mg\sin(\alpha_i + u_i') \tag{12}$$

where z_i $(i = 1,2,\ldots,m)$ is the relative displacement of the ith accelerometer and α_i $(i = 1,2,\ldots,m)$ is a constant denoting the angle between the vertical and the tangent to the structure in equilibrium at accelerometer location P_i. We assume that α_i $(i = 1,2,\ldots,m)$ can be computed from a static analysis. Using a small angle approximation in u_i', Eq. (12) becomes

$$m\ddot{w}_i + c\dot{w}_i + kw_i = -m\ddot{u}_i - mg(\cos\alpha_i)u_i' \tag{13}$$

where $w_i = z_i + mg\sin\alpha_i/k$ $(i = 1,2\ldots,m)$ denotes the motion of mass m in the ith accelerometer about its static equilibrium position. Note that for an accelerometer mounted vertically with $\alpha_i = \pi/2$ in Eq. (13), the dynamic effect of gravity is negligible. The dynamic effect of gravity is greatest for values $\alpha_i = 0$.

The accelerometer is a vibration-measuring instrument designed such that the excitation frequency ω is much smaller than the natural frequency ω_n of the accelerometer $\omega \ll \omega_n$, so that inertia and damping forces in Eq. (13) may be neglected because they are quite small in comparison to the elastic spring force of the accelerometer. Hence, Eq. (13) becomes

$$a_i = -\omega_n^2 w_i = \ddot{u}_i + g(\cos\alpha_i)u_i', \qquad i = 1,2,\ldots,m \tag{14}$$

where a_i represents the output of the ith accelerometer. Using Eqs. (9), (10), and (14), the accelerometer output a_i is given by

$$a_i = \sum_{r=1}^{\infty} \left\{ [g(\cos\alpha_i)\phi_r'(P_i) - \omega_r^2 \phi_r(P_i)] q_r(t) + \phi_r(P_i) f_r(t) \right\} \qquad i = 1,2,\ldots,m \tag{15}$$

where $\phi_r'(P_i)$ represents the slope of the rth mode of vibration at P_i. We consider the case of free vibration, i.e., $f_r(t) = 0$ $(r = 1,2,\ldots)$. At the accelerometer location P_i, where $g(\cos\alpha_i)\phi_r'(P_i) = \omega_r^2 \phi_r(P_i)$, the accelerometer output does not include the contribution to the acceleration of the rth mode. Hence, nodal accelerometer locations exist for modes of vibration that satisfy $g(\cos\alpha_i)\phi_r'(P_i) = \omega_r^2 \phi_r(P_i)$. Examining Eq. (15), for higher natural frequencies the effect of gravity may be negligible due to the domination of ω_r^2, so that accelerometer nodal locations occur predominantly in the lower modes of vibration.

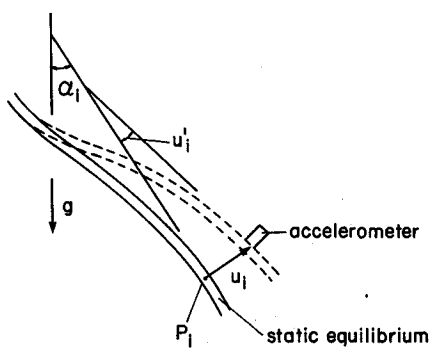

Fig. 4 Accelerometer mounted on a flexible structure in 1 g.

Observer Implementation

In this section, we develop an observer that uses accelerometer measurements as input. In general, the motion of a structure can be expressed as a linear combination of the lower modes of vibration, because a large amount of energy is required to excite the higher modes. We consider a modal observer comprising the lower modes of vibration.

The modal-state estimator has the form[7]

$$\dot{\hat{v}} = A\hat{v} + Bf + K(a - \hat{a}) \tag{16}$$

where

$$\hat{v} = [\hat{q}_1\ \hat{q}_2\ \dots\ \hat{q}_n\ \dot{\hat{q}}_1\ \dot{\hat{q}}_2\ \dots\ \dot{\hat{q}}_n]^T$$

is the modal-state estimate vector,

$$f = [f_1\ f_2\ \dots\ f_n]^T$$

is the modal force vector,

$$a = [a_1\ a_2\ \dots\ a_m]^T$$

and

$$\hat{a} = [\hat{a}_1\ \hat{a}_2\ \dots\ \hat{a}_m]^T$$

are the m-dimensional accelerometer output and estimated accelerometer output vectors, respectively, and A and B are plant matrices given by

$$A = \begin{bmatrix} 0 & I \\ -\Lambda & 0 \end{bmatrix}, \qquad B = \begin{bmatrix} 0 \\ I \end{bmatrix} \tag{17}$$

Note that I is the $n \times n$ identity matrix, 0 is an $n \times n$ null matrix, and Λ is an $n \times n$ diagonal matrix of eigenvalues corresponding to the lowest n modes of vibration. Furthermore, the matrix K is the observer gain matrix. If the system is treated as deterministic, Eq. (16) represents a Luenberger observer. If stochastic signals are considered, the gain matrix K may be designed to satisfy a Riccati equation, in which case Eq. (16) represents a Kalman filter.[15] The associated output equation has the form

$$\hat{a} = C\hat{v} + Df \tag{18}$$

where C and D are $m \times 2n$ and $m \times n$ dimensional matrices, respectively; from Eq. (15) their entries are given by

$$C_{rs} = 0, \qquad D_{rs} = \phi_s(P_r), \qquad r = 1,2,\dots,m$$

$$s = 1,2,\dots,n \tag{19a}$$

$$C_{rs} = g(\cos\alpha_r)\phi_s'(P_r) - \omega_s^2\phi_s(P_r), \qquad r = 1,2,\dots,m$$

$$s = n+1,\ n+2,\dots,2n \tag{19b}$$

A necessary condition for observability of the modal-estimator requires that the matrix C contain no more than n zero columns. The modal-state estimator gains K are designed so that the eigenvalues of the system

$$\dot{\epsilon} = (A - KC)\epsilon \tag{20}$$

lie in the left-half of the complex plane, in which $\epsilon = v - \hat{v}$ represents the state estimate error.

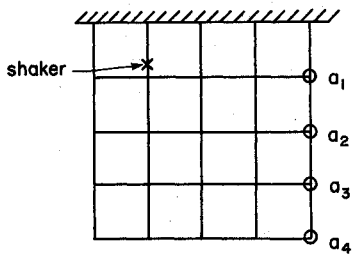

Fig. 5 AFAL Grid illustration.

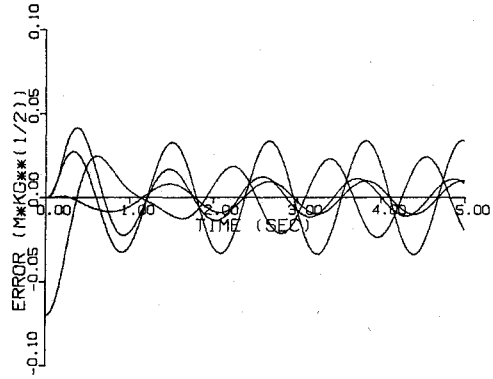

Fig. 6 Observer modal displacement estimation error: gravitational effects not included.

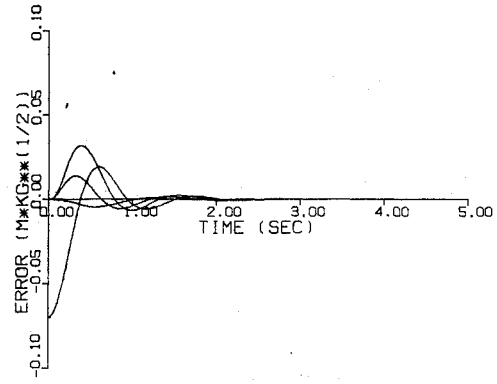

Fig. 7 Observer modal displacement estimation error: gravitational effects included.

Analytical and Experimental Results

To determine the effects of gravity on the accelerometer measurements, an observer was implemented for the AFAL Grid structure. The two-dimensional AFAL Grid structure is illustrated in Fig. 5. The observer was a modal-state estimator, given by Eqs. (16) and (17). The model used in the observer included the first four modes of vibration provided by a Nastran model of the grid structure. To test the observer, both analytical and experimental results were considered. In the analytical tests, the free response was used in which the plant and observer model contained no damping. For the experimental tests, damping was added to the first mode of vibration of the observer model. The amount of damping was determined experimentally. The structure was excited using an electromagnetic shaker with frequency approximately equal to the first natural frequency of the structure, so that the response consisted mainly of the first mode of vibration. Four accelerometers a_i (i = 1,2,3,4) and one shaker were placed as shown in Fig. 5, where the structure is suspended vertically so that $\alpha_i = 0$ (i = 1,2,3,4) in Eq. (19). The output equation for the observer is given by Eqs. (18) and (19).

We consider two cases for the observer in the analysis. In the first, the observer is constructed without the gravitational effect, i.e., $g = 0$ in Eq. (19), and in the second, the dynamic effect of gravity on the accelerometers is included in the observer design, i.e., $g = 9.81$ m/s^2 in Eq. (19). In both cases, the plant simulation includes the gravity effect on the accelerometers. The free response was used in which the plant simulation consisted of the first mode of vibration only. Figures 6 and 7 demonstrate the estimation error in the modal displacement ϵ_i (i = 1,2,3,4) for the first and second cases, respectively. Note that the estimation error shown in Fig. 6 does not approach zero. Examining Fig. 7, it is evident that the state estimation error converges to zero and that the effect of gravity must be included in the observer design, at least for estimation of the first mode of vibration of the grid structure.

Figure 8 presents experimental data, where the structure's response consisted mainly of the first mode of vibration due to the resonance excitation of the shaker. Note the apparent 180-deg phase shift between a_1 and the remaining accelerometer outputs, due to the incorrect sign of the output signal a_1. Moreover, Fig. 8 shows that the accelerometer nodal location for the first mode of vibration of the grid exists between a_1 and a_2, where these locations are illustrated in Fig. 5. The steady-state accelerometer outputs shown in Fig. 8 were used as input to the observer. It was necessary to add damping to the first mode of vibration of the observer, due to the resonance excitation of the structure. The damping added was experimentally observed for the first mode of vibration. The observer gains were computed using the solution of a Riccati equation with appropriate values for the noise intensities of the shaker and accelerometers, so that the observer is actually a Kalman filter.

For the experimental tests, we consider two cases for the Kalman filter, completely analogous to the simulation tests. In the first, the Kalman filter was constructed by ignoring the gravitational effect on the accelerometer output, using $g = 0$ in the output equation given by Eqs. (18) and (19). In the second case, the dynamic effect of gravity on the accelerometer output is included. The steady-state output for the Kalman filter design, ignoring gravity, is shown in Fig. 9. Note that the Kalman filter predicts the accelerometer outputs to be in phase, contrary to Fig. 8. To predict the sign and amplitude error caused by gravity in accelerometer a_1 and the amplitude error in the remaining accelerometers a_2, a_3, and a_4, we must include the dynamic effect of gravity on the accelerometers in the Kalman filter. The steady-state Kalman filter output, including gravity, is shown in Fig. 10. In this second case, the Kalman filter predicts a phase shift in accelerometer a_1, which is compatible with the experimental data. Comparing Figs. 8 and 10, we note that some disagreement must exist between the model and the actual structure, because the amplitudes of the accelerometer outputs predicted by the Kalman filter do not exactly match the experimental data.

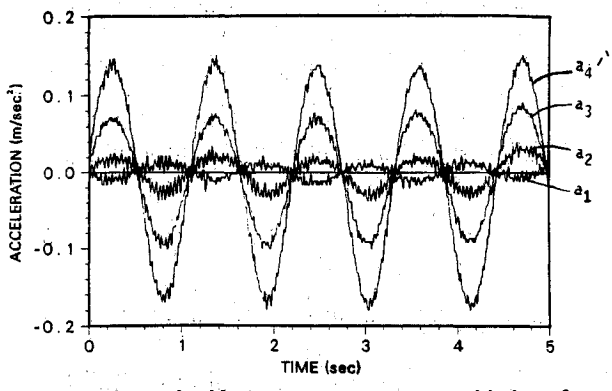

Fig. 8 Experimental grid response to resonance excitiation of mode 1.

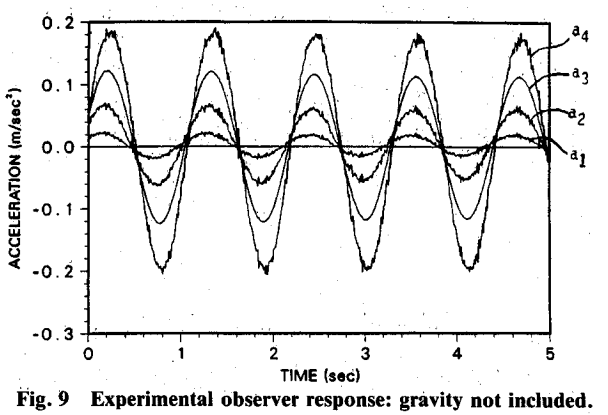

Fig. 9 Experimental observer response: gravity not included.

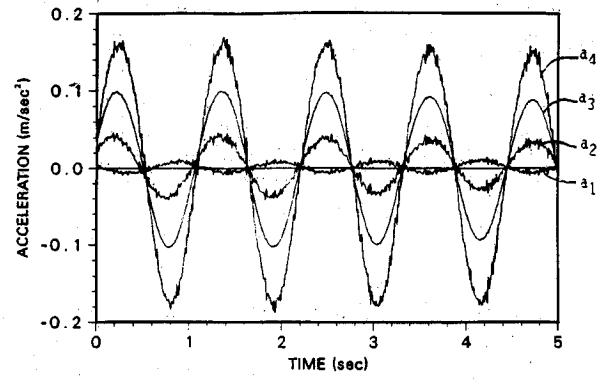

Fig. 10 Experimental observer response: gravity included.

Conclusions

Analytical and experimental results demonstrate the low-frequency response of accelerometers in a 1-g environment. It is concluded that for low-frequency response measurements, the dynamic effect of a uniform gravity field on the accelerometer signal cannot be ignored. The effect is demonstrated experimentally for pendulum motion and elastic vibration of the AFAL two-dimensional grid structure. Furthermore, the results of analysis and experiment show that accelerometer nodal locations exist, and predominantly occur in the lower modes of vibration. An observer is formulated to include the dynamic effect of gravity on the accelerometer measurements and is compared to an observer that ignores the effect of gravity. The observer is constructed for the AFAL Grid structure, and experimental results indicate that the dynamic effect of gravity on accelerometer measurements should be included in the observer design.

Acknowledgments

This work was supported by the Air Force Office of Scientific Research/Air Force Systems Command, U.S. Air Force, under Contract F49620-87-R-0004. The authors acknowledge the superb work performed by L. Carter of the Aerospace Engineering Department, Virginia Polytechnic Institute and State University, Blackburg, Virginia, in programming the simulations and generating some of the figures.

References

[1]Meirovitch, L. (ed.), *Proceedings of the First VPI&SU/AIAA Symposium on Dynamics and Control of Large Structures,* Virginia Polytechnic Inst. and State Univ., Blacksburg, VA, June 1977.

[2]Meirovitch, L. (ed.), *Proceedings of the Second VPI&SU/AIAA Symposium on Dynamics and Control of Large Structures,* Virginia Polytechnic Inst. and State Univ., Blacksburg, VA, June 1979.

[3]Meirovitch, L. (ed.), *Proceedings of the Third VPI&SU/AIAA Symposium on Dynamics and Control of Large Structures,* Virginia Polytechnic Inst. and State Univ., Blacksburg, VA, June 1981.

[4]Meirovitch, L. (ed.), *Proceedings of the Fourth VPI&SU/AIAA Symposium on Dynamics and Control of Large Structures,* Virginia Polytechnic Inst. and State Univ., Blacksburg, VA, June 1983.

[5]Meirovitch, L. (ed.), *Proceedings of the Fifth VPI&SU/AIAA Symposium on Dynamics and Control of Large Structures,* Virginia Polytechnic Inst. and State Univ., Blacksburg, VA, June 1985.

[6]Meirovitch, L. (ed.), *Proceedings of the Sixth VPI&SU/AIAA Symposium on Dynamics and Control of Large Structures,* Virginia Polytechnic Inst. and State Univ., Blacksburg, VA, June 1987.

[7]Balas, M. J., "Active Control of Flexible Systems," *Journal of Optimization Theory and Applications,* Vol. 25, No. 3, 1978, pp. 415–436.

[8]Das, A., Strange, T., Schlaegel, W., and Ward, J., "Experiment and Parameter Estimation of Flexible Structures," *Proceedings of the Second NASA/DOD CSI Technology Conference,* AFWAL-TR-88-3052, Final Rept., Nov. 1987, pp. 389–400.

[9]Wie, B., "Active Vibration Control Synthesis for the Control of

the Mast Flight System," *Journal of Guidance, Control and Dynamics,* Vol. 11, No. 3, 1988, pp. 271-277.

[10]Liebst, B. S., "Accelerometer Placement in Active Flutter Supression Systems," *Journal of Guidance, Control and Dynamics,* Vol. 10, No. 5, 1987, pp. 441-446.

[11]Meirovitch, L., *Elements of Vibration Analysis,* McGraw-Hill, New York, 1986, pp. 67-71.

[12]Vierck, R. K., *Vibration Analysis,* Harper & Row, New York, 1966.

[13]Doebelin, E. D., *Measurement Systems,* McGraw-Hill, New York, 1966.

[14]Meirovitch, L., *Computational Methods in Structural Dynamics,* Sijthoff & Noorhoff, Alpen aan den Rijn, the Netherlands, 1980.

[15]Junkins, J. L., *An Introduction to Optimal Estimation of Dynamical Systems,* Sijthoff & Noordhoff, Alpen aan den Rijn, the Netherlands, 1976.